Kneading theory of the circle map

E. Piña*
Departamento de Física, Universidad Autónoma Metropolitana—Iztapalapa, Apartado Postal 55-534, 09340 México, Distrito Federal, Mexico
(Received 23 September 1985)

The symbolic dynamics of the circle map $f_\lambda(x)=x+\lambda\sin(2\pi x)+a$ (mod 1) is analyzed with use of the symmetries of the lines $a=0$ and $a=\frac{1}{2}$, obtaining, by a projection method, factorization of the Artin-Mazur ζ function. The Milnor-Thurston kneading theory is shown to be of interest for both symmetric and nonsymmetric circle maps, where an obvious generalization is shown to be valid and certain calculations simplify the relationship between the Artin-Mazur ζ function and the itinerary.

I. INTRODUCTION

Nonlinear iterations of the interval or the circle have an important place in current scientific literature as methods for describing complex phenomena associated with nonlinear oscillations and recurrences in physics and other sciences.[1-19]

Differential equations are transformed into nonlinear difference equations, by using Poincaré maps,[1] the computer output of which has motivated many fruitful theorems and well-founded mathematical conjectures. The experimentalist relating these iteration models to the behavior of distinct physical systems have, in consequence, favored an exponential growth of mathematical research about the properties of nonlinear difference equations.

Period doubling and scaling are the two most attractive phenomena found in numerical and physical experiments (Refs. 1, 2, 10–12, and 14). Equally appealing is that the same sequence of periods is present in natural experiments and in computer iterations when the corresponding control parameter is increased.[5-7,9] Furthermore, the order of points in a periodic iteration, or of the maxima in a nonlinear oscillation are in correspondence and allow connection of the experimental oscillation with a one-dimensional map.[3-9]

Thus it is possible to predict the order of different kinds of oscillations and the qualitative characteristics of each when a parameter is tuned to the right value.

Striking examples are found in oscillations of periodic chemical reactions such as those of Belousov-Zhabotinskii or of the chlorite-thiosulfate.[5-8] Identical properties have been registered for electronic circuits including varactors,[9] all of which show remarkable parallelism to the behavior of one-dimensional maps.

The purpose of this paper is to extend previous work concerning maps of the interval[3,4] to maps of the circle

$$x_{n+1}=f_\lambda(x_n) \tag{1.1}$$

where n is a positive integer, x_n the value of the coordinate at the nth iteration, and f_λ a continuous iteration function of the circle depending on at least one real parameter λ. The symbolic dynamics used, though emphasizing new mathematical facts, were without any formal proof.

The prime example investigated was the mapping of the circle

$$x_{n+1}=x_n+\lambda\sin(2\pi x_n)+a \pmod 1, \quad 0\le a<1 \tag{1.2}$$

with a and λ being two parameters. This mapping has a long history, mainly of map behavior and properties when λ is small and the iteration function, monotonous (see Ref. 10 and citations therein).

The sine map has attracted much attention as a model in which interesting scaling phenomena observed in area-preserving maps of the plane are replicated.[10-12] A particular scaling occurs exactly at the value

$$\lambda=\tfrac{1}{2}\,, \tag{1.3}$$

where monotonicity is lost. A Cantor set in parameter space, known as the "devil's staircase," has been studied with renormalization-group principles by various authors[12] who affirm that the return map for a differential equation of the resistively-shunted Josephson junction is represented by a mapping of the circle.

Maps have also been used as models to represent the nonlinear intermittent oscillations to be witnessed in chemical reactions and in the phase locking of cardiac rhythms.[13] Numerical studies for large ranges of the two parameters have been analyzed by a number of workers.[13,14]

Our interest in the circle map (1.2) was first aroused upon observing that for $a=0$ and for small values of λ ($\lambda<0.732\,644\,13$), the circle map behaves similarly to the symmetric cubic map

$$z\to z+\lambda z(1-z)(\tfrac{1}{2}-z), \quad 4<\lambda\le 16 \tag{1.4}$$

as was previously reported in collaboration with Chavoya and Angulo.[4]

For the two we find a range of the parameter λ (distinct for each map) in which the very same order of periodic cycles is evident, as λ is increased. The order of points for each corresponding cycle also coincides.

The symmetry

$$f_\lambda(z)=1-f_\lambda(1-z) \tag{1.5}$$

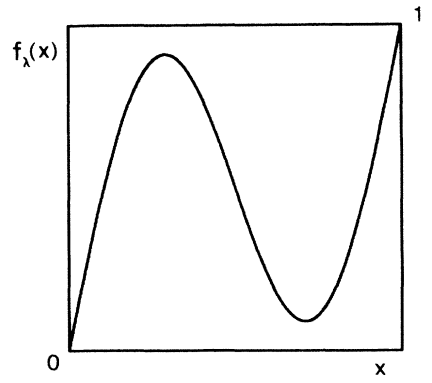

FIG. 1. $a=0$ sine map with no discontinuities; $\lambda=0.641\,62$.

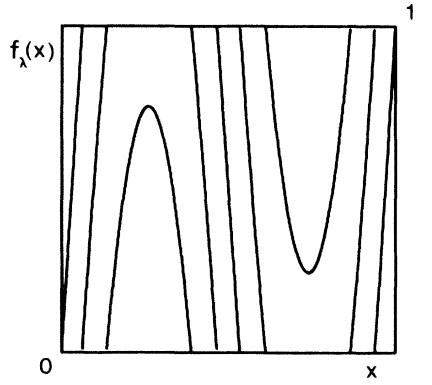

FIG. 3. $a=0$ sine map with eight discontinuities; $\lambda=2.5$.

is present in both maps and thus many interesting properties of the symmetric cubic map are incorporated into the $a=0$ circle map. Accordingly, much of the information previously obtained by Branner[15] and by Chavoya-Aceves *et al.*,[4] for continuous maps of the interval, can now be extended to the entire map of the circle for any value of the parameters by using similar techniques.

The $a=0$ sine map is used to illustrate a diffusive motion self-generated through a purely deterministic system.[16]

The map (1.2), for $a=\frac{1}{2}$, is symmetric, exhibiting property (1.5) as well. Most of the Branner's properties for symmetric cubics depend solely upon symmetry (1.5) and apply in this case. Following Branner,[15] the companion maps $g_\lambda(x)=f_\lambda(1-x)$,

$$x_{n+1}=-x_n-\lambda\sin(2\pi x_n) \pmod 1 \tag{1.6}$$

and

$$x_{n+1}=\tfrac{1}{2}-x_n-\lambda\sin(2\pi x_n) \pmod 1 \tag{1.7}$$

have behaviors which can be predicted from the $a=0$ and $\frac{1}{2}$, sine maps, respectively. Other consequences of this symmetry will be presented in the following sections.

The principal object of this paper is to predict the extension of the Milnor-Thurston kneading theory[17] to maps of the circle. Use of symmetry (1.5) was essential before considering general nonsymmetric cases. The Milnor-Thurston work in the main case affords an elegant view of the symbolic dynamics of a continuous map of the interval. However, their ideas can validly be extended to the circle map as well. In this paper the continuous map of the circle (1.2) is regarded as a noncontinuous map of the interval with a finite number of discontinuities of which the only sort permitted are called periodic boundary conditions, as shown in Figs. 1–8. Section IV presents, for the case of the circle maps, the expression for the Milnor-Thurston kneading determinant, which is equal to the inverse of the Artin and Mazur ζ function.

II. SYMBOLIC DYNAMICS

Before extending results, a brief survey the idea to be generalized will be provided. For certain values of the parameter stable periodic cycles of period p are found characterized by the properties

$$\lim_{n\to\infty} f_\lambda^{(np)}(x)=y\ , \tag{2.1}$$

$$f_\lambda^{(p)}(y)=y\ , \tag{2.2}$$

and

$$|f_\lambda'^{(p)}(y)|<1\ , \tag{2.3}$$

where $f_\lambda^{(n)}$ represents the nth iterate of function f_λ, x a generic initial condition, and y the limit value for the smaller p. The p iterates

$$f_\lambda^{(j)}(y)=y_j \quad (j=1,\ 2\ ,\ \ldots\ ,\ p) \tag{2.4}$$

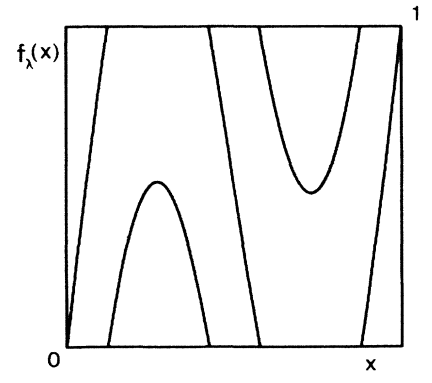

FIG. 2. $a=0$ sine map with four discontinuities; $\lambda=1.2582$.

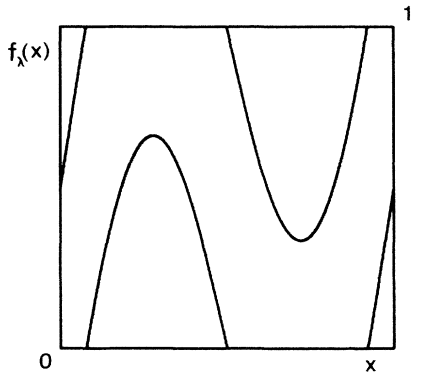

FIG. 4. $a=\frac{1}{2}$ sine map with three discontinuities; $\lambda=0.9$.

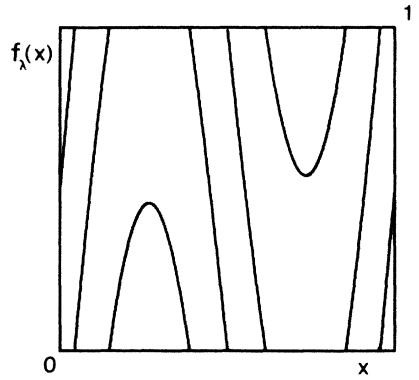

FIG. 5. $a=\frac{1}{2}$ sine map with seven discontinuities; $\lambda=1.7$.

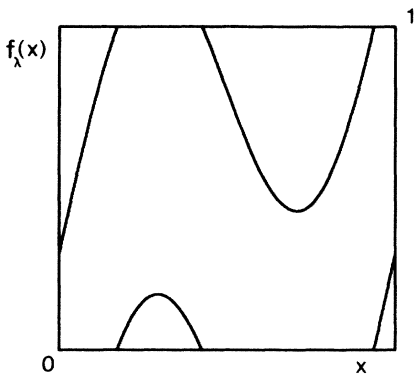

FIG. 7. Nonsymmetric sine map with three discontinuities; $a=0.3$, $\lambda=0.6$.

form a cycle of period p for a particular value of the parameter λ. Iterating the maps (1.2) and (1.4) it is possible to find one stable cycle or two coexisting stable cycles. By changing the value of the parameter λ, a good many other cycles are found. By means of a precise formulation these cycles may be ordered in correspondence with the relative magnitude of the parameter λ.

In the maps considered here the stable cycles become unstable as Eq. (2.3) is violated at a bifurcation value of the parameter λ. Equations (2.2) and (2.4) define the unstable periods even though (2.1) and (2.3) are no longer satisfied.

The stable cycles are born by bifurcation at a λ value of the parameter. The number of unstable cycles grows with λ. However, for lower values of λ, cycles neither stable nor unstable are present.

The number of unstable cycles of any period coexisting with a particular stable cycle are determined by the Artin-Mazur function[20]

$$\zeta(t)=\exp\sum_j N_j t^j/j\ , \tag{2.5}$$

which is the generating function for the number N_j of periodic unstable points of period j, including the divisors of j.

A model of constructing this function for a given stable cycle which follows from the permutation and the Stefan matrices is now given: First, to obtain the permutation matrix, we number all the points (2.4) in the cycles (one or two stable cycles) to correspond to the values of the coordinate y_j in the interval or cycle, and we write the permutation resulting from iteration with f_λ,

$$\begin{bmatrix} 1 & 2 & \cdots & T \\ a_1 & a_2 & \cdots & a_T \end{bmatrix}. \tag{2.6}$$

This symbol, representing the permutation of integers 1 to T, implies that a_j is the ordinal of the coordinate obtained by iterating the jth coordinate.

The permutation (2.6) exhibits two important properties: The first, the shape of the iteration function is represented by numbers $a_1,a_2,\ldots,a_T$. This, a general property of mappings, was earlier pointed out for quadratic and cubic maps. For the cubic and the $a=0$ sine map, the numbers a_j in the permutation (2.6) grow up to the maximum T, then decrease to the minimum 1, and again grow, thus reproducing the slopes of the sinusoidal iteration functions.

This convenient property is useful in relating the allowed permutation with the iteration function. The shape of an experimental permutation or cycle should be in agreement with that of the map if it is used to formally represent that oscillation. A print mistake in nonlinear oscillations of chemical reactions[5] was found in this way.[21] One example of coexisting bistable cycles of period four is

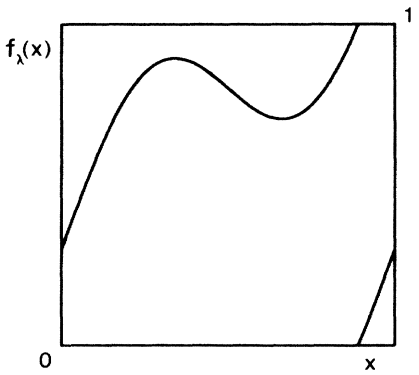

FIG. 6. Nonsymmetric sine map with one discontinuity; $a=0.3$, $\lambda=0.3$.

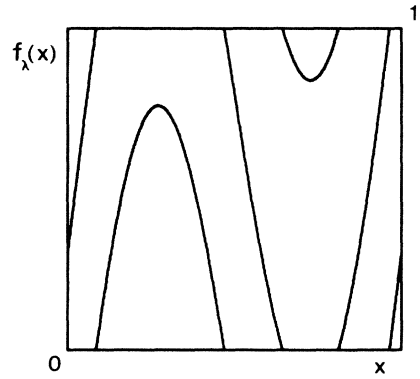

FIG. 8. Nonsymmetric sine map with five discontinuities; $a=0.3$, $\lambda=1$.

$$\begin{bmatrix} 1 & 2 & 3 & 4 & 5 & 6 & 7 & 8 \\ 5 & 6 & 8 & 7 & 2 & 1 & 3 & 4 \end{bmatrix} . \tag{2.7}$$

The second important property of the permutation (2.6) arises in the presence of a symmetry. The numbers a_j in the case of the symmetry (1.5) obey the equation

$$a_j + a_{d+1-j} = d + 1 , \tag{2.8}$$

where d is the dimension of the permutation matrix, 8 in example (2.7).

The dynamics of the intervals between the periodic points permitted by matrix (2.6), are represented by a Stefan matrix describing the image intervals of each interval under iteration.[3,4,18]

The Stefan matrix mimics the graph of the iteration function (adding, however, a vertical inversion) with groups of the number one blocked into columns and separated each from the other by vertices in the position of the nonzero entries of the permutation matrix.[3,4] This property is generalized for the circle map.

If $\underline{A}$ is the Stefan matrix, then the periodic points N_p are equal to the trace of $\underline{A}$ to the p power

$$N_p = \text{trace}(\underline{A}^p) . \tag{2.9}$$

Geometrically, this property coincides with the location of the fixed points of a function by means of the intersection of its graph with a straight line bisecting the coordinate axes.

Thus the Artin-Mazur ζ function is obtained from the characteristic determinant of matrix $\underline{A}$

$$1/\zeta(t) = |\underline{1} - \underline{A}t| = 1 - \sum_{j=1}^{d} \alpha_j t^j , \tag{2.10}$$

where α_j are the coefficients of the characteristic polynomial

$$P_A(x) = x^d - \sum_{j=1}^{d} \alpha_j x^{d-j} . \tag{2.11}$$

We resort to these coefficients to evaluate the periodic unstable points by the linear iteration[3,4]

$$N_k = \sum_{j=1}^{d} \alpha_j N_{k-j} . \tag{2.12}$$

A factorization of the characteristic polynomial (which is equivalent to that of the Artin-Mazur function) is obtained for the symmetry of the Stefan matrix in the symmetric cubic.[4]

The eigenvectors of this matrix fall into even and odd eigenvectors with respect to inversion $j \leftrightarrow N+1-j$ of the index of its entries. Even and odd both belonging to orthogonal spaces. This splitting is the reason for the factorization.

The Branner's companion mapping[15] of a symmetric map also has the symmetry and factorization of a cubic. In fact, at the same value of the parameter, it is possible to find Stefan matrices differing only in a vertical inversion for both maps. The eigenvectors, therefore, are identical. While the eigenvalues of even vectors are the same, the eigenvalues of odd vectors differ in sign. An identical polynomial factor is also found in the characteristic polynomial with roots of even eigenvectors. The odd polynomial factor is different only in the sign of the odd powers.

The factorization can also be considered as the result of symmetry in the Milnor-Thurston kneading determinant,[17] since symmetry, as explained in Sec. IV, produces either a common factor in a column or a difference of squares of two polynomials.

III. SYMBOLIC DYNAMICS OF THE CIRCLE MAP

The analogous behavior of the symmetric cubic and the $a=0$ sine map, provides many ideas with which to generalize upon the symbolic dynamics of the interval to the circle maps. An outstanding difference between the dynamics of the circle map and the maps of the interval is that of the identification of the points 0 and 1. In the circle this point joins the two subintervals at the extrema, forming a single subinterval.

Accordingly, we must suppress a row and a column of the Stefan matrices to allow for the 0, 1 identification. Thus the characteristic polynomial will differ by a lost factor $(x-1)$, corresponding to this identification. The Branner's companion map (1.6), on the other hand, will have gained a new fixed point, and a new factor $(x-1)$, when this identification is made.

To illustrate the changes in the Stefan matrix occurring from the cubic to the circle, we take, for example, the period corresponding to symbol MRC of the symmetric cubic[4] at value $\lambda = 14.801\,262$. This period is found for the $a=0$ sine map at $\lambda = 0.641\,62\ldots$ (see Fig. 1).

Thus the Stefan matrices for both maps become, respectively,

$$\begin{bmatrix} 1&0&0&0&0&0&0 \\ 1&0&0&0&1&1&0 \\ 1&0&0&1&0&1&0 \\ 0&1&0&1&0&1&0 \\ 0&1&0&1&0&0&1 \\ 0&1&1&0&0&0&1 \\ 0&0&0&0&0&0&1 \end{bmatrix} , \quad \begin{bmatrix} 0&0&0&1&1&1 \\ 0&0&1&0&1&1 \\ 1&0&1&0&1&0 \\ 1&0&1&0&0&1 \\ 1&1&0&0&0&1 \\ 0&0&0&0&0&1 \end{bmatrix} . \tag{3.1}$$

Note that the first row and first column of the cubic have each been suppressed in the sine matrices, and that the last column of the sine matrix is transformed to incorporate two number ones in the first column of the cubic's. Only the first number 1 on the diagonal of the cubic matrix is lost for it has become identified with the final 1.

The graph of the iteration function is recovered in the maps of the interval by the Stefan matrix. It is possible to do likewise for maps of the circle by constructing a tiling with the Stefan matrix, as shown in Fig. 9. It often happens that for continuity the last column of one tile is extended over into that of the next. This effect on the border of the matrix could be equally obtained by defining the Stefan matrices of a circle map onto a torus when we join the parallel edges of the matrix.

The entry S_{ij} of a Stefan matrix is equivalent to the number of times the interval j is included in the image of

the interval i. For the quadratic or cubic functions previously studied[3,4] this number is invariably 1. However, for the circle map this value can be otherwise (not 1 but a positive integer).

In any case, the Stefan matrix reproduces the graph of the function and an integer as entry equals the number of lines of the iteration function represented by that entry. These lines should be continued into a neighboring entry.

To illustrate, the Stefan matrix of the cycle occurring for values of the parameters $a=0$ and $\lambda=1.2582$,

$$\begin{bmatrix} 1 & 0 & 0 & 1 & 0 & 3 \\ 1 & 0 & 1 & 0 & 0 & 3 \\ 1 & 0 & 1 & 0 & 1 & 4 \\ 0 & 0 & 1 & 0 & 1 & 3 \\ 0 & 1 & 0 & 0 & 1 & 3 \\ 0 & 1 & 0 & 1 & 0 & 3 \end{bmatrix}, \tag{3.2}$$

should be compared with the graph of the sine map for the same values of the parameters in Fig. 2.

In the tiles similar to those of Fig. 9, half turn symmetries around any one of the two entries S_{33} and S_{66} were observed. A property which is general to the maps of the circle with symmetry (1.5), is represented in matrix algebra by a rotation matrix $\underline{R}$, commuting with the Stefan matrix

$$\underline{R}\,\underline{S}=\underline{S}\,\underline{R}\ , \tag{3.3}$$

where matrix $\underline{R}$ is defined by

$$R_{ij}=\delta(i+j)=\begin{cases} 1 & \text{when } i+j=d \text{ or } 2d \\ 0 & \text{otherwise}\ , \end{cases} \tag{3.4}$$

d being the dimension of matrices $\underline{R}$ and $\underline{S}$. The matrix $\underline{R}$ is well known in applied mathematics as the square of the discrete Fourier transform.[22]

Matrix $\underline{R}$ is its own inverse, and defines two projectors

$$(\underline{1}\pm\underline{R})/2\ , \tag{3.5}$$

splitting the eigenvector space of the Stefan matrix into even and odd subspaces. The even vectors of the matrix $\underline{S}$ are also eigenvectors of the projector $(\underline{1}+\underline{R})/2$ with eigenvalue 1, and odd eigenvectors of $\underline{S}$ are eigenvectors of projector $(\underline{1}-\underline{R})/2$ with eigenvalue -1.

Factorization of the characteristic polynomial of the Stefan matrix produces factorization of the Artin-Mazur ζ function as well. Two factors being found: one, the ζ function of the matrix $\underline{S}(\underline{1}+\underline{R})/2$; the other, the ζ function of $\underline{S}(\underline{1}-\underline{R})/2$.

The above-mentioned factorization was previously encountered and reported in our study of the cubic map.[4] This factorization could be a particular application of the Milnor-Thurston kneading theory. Here, however, it results from symmetry (1.5), and becomes therefore valid for larger values of the parameter λ, which when considered as a map of the interval shows discontinuities of the iteration function. Thus the Milnor-Thurston theory should be restated.

At value $a=\frac{1}{2}$ the same factorization is found for the sine map. In this case the symmetry (1.5) is also valid and

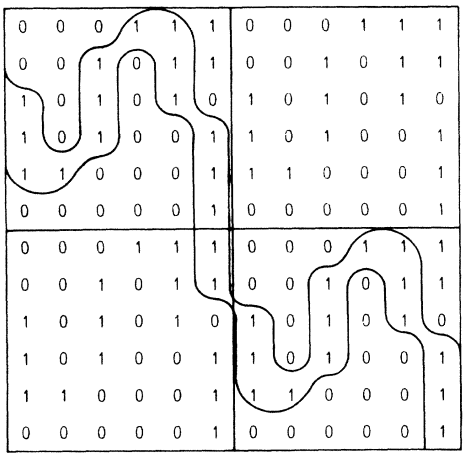

FIG. 9. Four tiles of a Stefan matrix of the $a=0$ sine map.

once again factorization of the Artin-Mazur function follows.

Since factorization of the characteristic polynomial of matrix $\underline{S}$ is easily obtained from the known projectors (3.5), an analysis of the Artin-Mazur function was undertaken in search of a simple relation which was discovered in the cubic map with the itinerary. If symmetry is included, this relation is identifiable with the Milnor-Thurston kneading determinant. The results of this study exemplify the kneading theory of the circle map presented in Sec. IV. The companion maps [(1.6) and (1.7)] of these symmetric sine maps having identical symmetry are analyzed similarly.

IV. KNEADING OF THE CIRCLE MAPS

Presented in this section is a pragmatic version of the Milnor-Thurston kneading theory,[17] and the suggestion made as to how it should be further generalized to explain the hundredfold output of distinct stable cycles of the circle map. The suggestion does not bear upon the complete and formally correct theory, but on a simplified algorithm to compute readily the Artin-Mazur ζ function.

To begin with, we examine the case $a=0$. The sine for $\lambda<0.7326$ behaves as a map of the interval and therefore the Milnor-Thurston theory directly applies. The fundamental assumption in the Milnor-Thurston kneading theory is the separation of the interval into the largest subintervals continuous and monotonous (laps). The points separating contiguous laps are at the extrema (maxima and minima) of the iteration function. Two extrema and three laps are had for the cubic map and for the sine map without discontinuities. The subintervals separated by the extrema are designed as I_j $(j=1,2,3)$ and the extrema, as E_k $(k=1,2)$.

For most of the values of the parameters, iteration of any extrema leads eventually to an asymptotic periodic attractor of period p. Two cases are then possible.

(1) Iteration of the two extrema will lead to distinct cycles. We call these bistable.

(2) The two iterations of the extrema will be attracted to the same limit cycle designed as an isolated cycle.

Iterating with the p-iterated function $f_\lambda^{(p)}$ of the extrema, we identify the limit points associated with the extrema. They are stable periodic points closest to the extrema.

We denote the points associated with the maximum and the minimum as M and m, respectively, and through iteration of those points the cycles

$$y_j = f_\lambda^{(h)}(M) \tag{4.1}$$

and

$$z_j = f_\lambda^{(j)}(m) \tag{4.2}$$

are obtained. In the first case, the two periods p and q are such that

$$M = f_\lambda^{(p)}(M), \quad m = f_\lambda^{(q)}(m) . \tag{4.3}$$

In the second case of an isolated cycle of period $p+q$, the same letters p and q for the number of periodic points between extrema become

$$M = f_\lambda^{(p)}(m), \quad m = f_\lambda^{(q)}(M) . \tag{4.4}$$

In presence of symmetry $p=q$; p could, in general, be different from q.

For a cycle, the address A will denote the lap of the set $\{I_k\}$ containing the j iterate (4.1) of M. B_j will denote the lap containing the j iterate (4.2) of m, and formally define the last address ($j=p$) as the average of the intervals on both sides of the extrema in play

$$A_p = \begin{cases} (I_1+I_2)/2 & \text{if } p \text{ corresponds to the maximum} \\ (I_2+I_3)/2 & \text{if } p \text{ corresponds to the minimum} . \end{cases} \tag{4.5}$$

Similarly, B_q will be defined as a formal average of the intervals on both sides of the extrema at the qth place following m. Moreover, $A_0^{\pm}$ and $B_0^{\pm}$ will be defined by

$$A_0^- = I_1, \quad A_0^+ = I_2$$

and (4.6)

$$B_0^- = I_2, \quad B_0^+ = I_3 .$$

The sequence $A_0^{\pm}, A_1, A_2, \ldots, A_p$ is known as the itinerary of the maximum, and the sequence $B_0^{\pm}, B_1, B_2, \ldots, B_q$, the itinerary of the minimum.

Now assigning a sign to each lap

$$\epsilon(I_j) = \begin{cases} 1 & \text{when } f_\lambda \text{ is monotonous increasing in } I_j \\ -1 & \text{when } f_\lambda \text{ is monotonous decreasing in } I_j . \end{cases} \tag{4.7}$$

Next, consider the invariant coordinate of the extrema as

$$\Theta_M(t) = \sum_{j=0}^{p} A_j t^j \prod_{k=1}^{j-1} \epsilon(A_j) \tag{4.8}$$

and

$$\Theta_M(t) = \sum_{j=0}^{p} B_j t^j \prod_{k=1}^{j-1} \epsilon(B_j) . \tag{4.9}$$

The invariant coordinate has been used for ordering points in a cycle[17] and for arranging cycles as a function of parameters.[4]

The kneading invariant measures the discontinuity of the invariant coordinate at the extrema according to the $+$ or $-$ laps at (4.6) used,

$$\Theta_M^+(t) - \Theta_M^-(t) = 2\Theta_M^+(t) - A_0^+ - A_0^- = \sum_{j=1}^{3} P_j(t) I_j , \tag{4.10}$$

where polynomials $P_j(t)$ are formed with the terms multiplying the corresponding lap I_j. The kneading invariant associated with the minima is

$$\Theta_m^+(t) - \Theta_m^-(t) = 2\Theta_m^+(t) - B_0^+ - B_0^- = \sum_{j=1}^{3} Q_j(t) I_j , \tag{4.11}$$

where $Q_j(t)$ are the polynomials formed with the terms multiplying the corresponding laps.

The kneading matrix is formed with polynomials $P_j(t)$ and $Q_j(t)$,

$$\begin{bmatrix} P_1(t) & P_2(t) & P_3(t) \\ Q_1(t) & Q_2(t) & Q_3(t) \end{bmatrix} . \tag{4.12}$$

The symmetry (1.5) of the $a=0$ sine map induces the property

$$P_j(t) = -Q_{4-j}(t) .$$

The kneading matrix annihilates the vector $1-\epsilon(I_j)t$ and, therefore,

$$\sum_j P_j(t)[1-\epsilon(I_j)t] = 0 . \tag{4.13}$$

The kneading determinant is the inverse of the Artin-Mazur ζ function obtained by suppressing the final column of the kneading matrix

$$\begin{aligned} 1/\zeta(t) &= P_2(t)[P_3(t) - P_1(t)] \\ &= [P_3(t) - P_1(t)][P_3(t) + P_1(t)] \\ &\quad \times (t-1)/(t+1) , \end{aligned} \tag{4.14}$$

where the last equation obtained takes into account the orthogonal property (4.13).

Thus the itinerary of the extrema may be used to calculate the Artin-Mazur ζ function. In the case of the cubic map these results are obtained as empirical rules deduced directly from the itineraries and the factorization of the characteristic polynomials of the Stefan matrices,[4] independently of the Milnor-Thurston papers.

While the generalization of the Milnor-Thurston kneading theory for the circle suffices for the examples considered, the theory should be extended for the reason that maps of the circle viewed as such are continuous, but become discontinuous if viewed as maps of the interval. (See Figs. 1–8.)

The Milnor-Thurston algorithm to construct the Artin-Mazur ζ function remains nearly the same. When the map of the circle is considered as a map of the interval, the points of discontinuity are incorporated as turning

points separating different laps. The subinterval including the origin is considered as two distinct subintervals or laps.

At first sight any particular case seems cumbersome. For example, the map of the circle for the values given in Fig. 3 comprises eight discontinuities, ten turning points, and a kneading matrix with 110 functions all to be considered. The kneading determinant requires the carrying out of 10! operations with polynomials in order to be able to calculate the Artin-Mazur function. Actually, this function can be obtained with the same formal result in plenty of cases. This result will come from using well-known properties of determinants in the kneading determinant.

After the first laps visited, the iteration of discontinuities follows the same itinerary. For itineraries of extrema, the only case presented in Milnor-Thurston papers, the different slopes of each side of laps joining at the extrema produces a term in the kneading invariant from each lap in the itinerary. For discontinuities this is no longer true; the slopes do not change sign at a discontinuity. Most laps of the itinerary for these discontinuities do not affect the kneading matrix. When it happens that an iteration of discontinuities falls at the extrema things change for the kneading matrix. Yet this case is simplified in the kneading determinant. Since the occurrence for the itinerary of that extrema has already been considered in the determinant it is not necessary to include its repetition in the itinerary of the discontinuity. Hence, only the first laps of the itineraries of discontinuities are considered.

When the polynomials of the itineraries of the extrema are formally written, all the periodic cycles with an equal number of discontinuities have similar kneading determinant.

Calculation of the kneading determinant for the non-symmetric circle maps leads to

$$\frac{1}{\zeta(t)}=(1-t)^{-1}\begin{vmatrix} \sum_j L_j(t)+t\left[-\sum_j jL_j(t)+\sum_j jC_j(t)-\sum_j jR_j(t)\right] & \sum_j C_j(t) \\ \sum_j \tilde{L}_j(t)+t\left[-\sum_j j\tilde{L}_j(t)+\sum_j j\tilde{C}_j(t)-\sum_j j\tilde{R}_j(t)\right] & \sum_j \tilde{C}_j(t) \end{vmatrix}, \tag{4.15}$$

where $L_j(t)$, $C_j(t)$, and $R_j(t)$ are the polynomials that multiply the laps forming the kneading invariant in Eq. (4.10), and where the tilde denotes the polynomials in Eq. (4.11). In the case of the circle map the polynomials to the left of the maximum are designated by the letter L, with the subindex ordering the laps. Starting from subindex zero the index increases toward the right. The $C_j(t)$ are the polynomials between extrema. The index is identical for both sides of the maximum and decreases toward the right. The $R_j(t)$ polynomials correspond to the laps to the right of the minimum, the rightmost lap with subindex zero (when $a=0$) or minus one (when $a=0$). The index decreases toward the left. For example, polynomials of the map drawn in Fig. 5 should be denoted $L_0,L_1,L_2,C_2,C_1,C_0,C_{-1},R_{-2},R_{-1},R_0$.

Notation has been selected to obtain expression (4.15) independently valid of the number of discontinuities, and representing symmetric cases $a=0$ and $\frac{1}{2}$ by adding the symmetry constraints valid for $a=0$,

$$\begin{aligned} \tilde{R}_{-1-k}(t)&=-L_k(t)\,,\\ \tilde{L}_k(t)&=-R_{-1-k}(t)\,,\\ \tilde{C}_k(t)&=-C_{-k}(t)\,, \end{aligned} \tag{4.16}$$

and the symmetry constraints valid for $a=\frac{1}{2}$,

$$\begin{aligned} \tilde{L}_j(t)&=-R_{-j}(t)\,,\\ R_{-j}(t)&=-L_j(t)\,,\\ \tilde{C}_j(t)&=-C_{1-j}(t)\,. \end{aligned} \tag{4.17}$$

Based on this notation, (4.13) is written

$$(1-t)\sum_j [L_j(t)+R_j(t)]+(1+t)\sum_j C_j(t)=0\,. \tag{4.18}$$

Taking into account symmetry constraints, the ζ function of the $a=0$ symmetric case is

$$1/\zeta(t)=\left[\sum_j [L_j(t)+R_j(t)]\right]\left[\sum_j [L_j(t)-R_j(t)]-t\sum_j (2j+1)[L_j(t)+R_j(t)]+2t\sum_j jC_j(t)\right]\Big/(1+t)\,. \tag{4.19}$$

And the ζ function of the symmetric $a=\frac{1}{2}$ result in the form

$$1/\zeta(t)=\left[\sum_j [L_j(t)+R_{-j}(t)]\right]\left[\sum_j [L_j(t)-R_{-j}(t)]-2t\sum_j j[L_j(t)-R_{-j}(t)]+t\sum_j C_j(t)(2j-1)\right]\Big/(1+t)\,. \tag{4.20}$$

These results were verified for hundreds of cases by direct computation of the symmetric and nonsymmetric circle map.

The premises upon which these studies have been based have been applied to other mappings and return maps. One case of particular interest is the Lorenz model[23,1] as studied by Birman and Williams[24] based on the knot theory in which they used a return map of two laps represented by the letters x and y. This is a monotonic and discontinuous map, and the kneading theory predicts if $P(x)$ is the polynomial of any permutation cycle of this map, then $P(x)(x-2)/(x-1)$ is the polynomial of its Stefan matrix. Another way of obtaining this result is by straightforwardly taking the discrete Fourier transform of the Stefan matrix.

ACKNOWLEDGMENTS

I wish to thank Mrs. L. Jiménez and Mr. O. Chavoya-Aceves for their help with the computation and Dr. Rafael Pérez, Professor L. Glass, and Professor J. Guckenheimer for their useful comments and observations.

---

*Also at Instituto Nacional de Investigaciones Nucleares, México, Distrito Federal, Mexico.

[1]J. Guckenheimer and P. Holmes, *Nonlinear Oscillations, Dynamical Systems, and Bifurcations of Vector Fields* (Springer-Verlag, New York, 1983).

[2]P. Collet and J. P. Eckman, *Iterated Maps on the Interval as Dynamical Systems* (Birkhauser, Basel, 1980).

[3]E. Piña, in *Lecture Notes in Physics*, edited by K. B. Wolf (Springer, Berlin, 1983), Vol. 189, p. 402.

[4]O. Chavoya-Aceves, F. Angulo-Brown, and E. Piña, Physica D **14**, 374 (1985).

[5]R. H. Simoyi, A. Wolf, and H. L. Swinney, Phys. Rev. Lett. **49**, 245 (1982).

[6]H. L. Swinney, Physica D **7**, 3 (1983).

[7]J.-C. Roux, Physica D **7**, 57 (1983).

[8]J. Maselko and I. R. Epstein, J. Chem. Phys. **80**, 3175 (1984).

[9]J. Testa, J. Perez, and C. Jeffries, Phys. Rev. Lett. **48**, 714 (1982).

[10]D. Rand, S. Ostlund, J. Sethna, and E. Siggia, Phys. Rev. Lett. **49**, 132 (1982); S. Ostlund, D. Rand, J. Sethna, and E. Siggia, Physica D **8**, 303 (1983).

[11]S. J. Shenker, Physica D **5**, 405 (1982); M. J. Feigenbaum, L. P. Kadanoff, and S. J. Shenker, *ibid.* **5**, 370 (1982); L. P. Kadanoff, J. Stat. Phys. **31**, 1 (1983); B. I. Schraiman, Phys. Rev. A **30**, 1970 (1984); R. S. Mackey and C. Tresser (unpublished); J. D. Farmer and I. I. Satija, Phys. Rev. A **31**, 3520 (1985).

[12]M. H. Jensen, P. Bak, and T. Bohr, Phys. Rev. Lett. **50**, 1637 (1983); Phys. Rev. A **30**, 1960 (1984); T. Bohr, P. Bak, and M. H. Jensen, *ibid.* **30**, 1970 (1984); O. E. Lanford III, Physica D **14**, 403 (1985); P. Bak and M. H. Jensen (unpublished); M. H. Jensen, T. Bohr, P. V. Christiansen, and P. Bak (unpublished).

[13]L. Glass and R. Perez, Phys. Rev. Lett. **48**, 1772 (1982); R. Perez and L. Glass, Phys. Lett. **90A**, 441 (1982); L. Glass, M. R. Guevara, A. Schrier, and R. Perez, Physica D **7**, 89 (1983); L. Glass, M. R. Guevara, J. Belair, and A. Schrier, Phys. Rev. A **29**, 1348 (1984).

[14]K. Kaneko, Prog. Theor. Phys. **68**, 669 (1982); M. Schell, S. Fraser, and R. Kapral, Phys. Rev. A **28**, 373 (1983); S. Fraser and R. Kapral, Phys. Rev. A **30**, 1017 (1984).

[15]Bodil Branner, J. Math. Anal. Appl. **105**, 276 (1985).

[16]T. Geisel and J. Nierwetberg, Phys. Rev. Lett. **48**, 7 (1982).

[17]J. W. Milnor and W. P. Thurston (unpublished).

[18]S. Smale and R. Williams, J. Math. Biol. **3**, 1 (1976); J. Guckenheimer, G. Oster, and A. Ipaktchi, *ibid.* **4**, 101 (1977); B. Derrida, A. Gervois, and Y. Pomeau, Ann. Inst. Henri Poincaré A **29**, 305 (1978).

[19]E. Piña, Phys. Rev. A **30**, 2132 (1984).

[20]M. Artin and B. Mazur, Ann. Math. **81**, 82 (1965).

[21]H. L. Swinney (private communication).

[22]L. Auslander and R. Tolmieri, Bull. Am. Math. Soc. **1**, 847 (1979).

[23]E. N. Lorenz, J. Atmos. Sci. **20**, 130 (1963).

[24]J. S. Birman and R. F. Williams, Topology **22**, 47 (1983).